AIMS Mathematics, 8(3): 5588–5615.
DOI: 10.3934/math.2023282
Received: 23 October 2022
Revised: 20 November 2022
Accepted: 20 November 2022
Published: 20 December 2022

http://www.aimspress.com/journal/Math

Research article

Multi-fractional-differential operators for a thermo-elastic magnetic response in an unbounded solid with a spherical hole via the DPL model

Osama Moaaz[1,*] and Ahmed E. Abouelregal[2,3,*]

[1] Department of Mathematics, College of Science, Qassim University, P.O. Box 6644, Buraydah 51452, Saudi Arabia
[2] Department of Mathematics, College of Science and Arts, Jouf University, Al-Qurayyat 77455, Saudi Arabia
[3] Department of Mathematics, Faculty of Science, Mansoura University, Mansoura 35516, Egypt

*** Correspondence:** Email: o.refaei@qu.edu.sa; ahabogal@ju.edu.sa.

Abstract: The current research aims to investigate thermodynamic responses to thermal media based on a modified mathematical model in the field of thermoelasticity. In this context, it was considered to present a new model with a fractional time derivative that includes Caputo-Fabrizio and Atangana-Baleanu fractional differential operators within the framework of the two-phase delay model. The proposed mathematical model is employed to examine the problem of an unbounded material with a spherical hole experiencing a reduced moving heat flow on its inner surface. The problem is solved analytically within the modified space utilizing the Laplace transform as the solution mechanism. An arithmetic inversion of the Laplace transform was performed and presented visually and tabularly for the studied distributions. In the tables, specific comparisons are introduced to evaluate the influences of different fractional operators and thermal properties on the response of all the fields examined.

Keywords: Multi-fractional operators; DPL model; phase lags; spherical hole; moving heat flow
Mathematics Subject Classification: 35B40, 35Q79, 35J55, 45F15, 73B30

1. Introduction

One of the most significant challenges in materials and hard sciences is finding an adequate theoretical formulation that effectively describes the behavioral responses of the materials in

question. The characteristics of these materials from a purely physical standpoint are of special interest to investigators. The mathematical modeling leads to conclusions completely in line with the experiment results. Several decades ago, fractional calculus, previously thought of as a branch of pure mathematics, was discovered to be of great value and has many applications in various fields of investigation and analysis. It is used to represent a variety of natural and physical processes. Among those applications are those used in models of neural networks, electrodes, bioengineering, and mathematical biology and their implications. This important area of mathematics is also used in economics and business, electrical and mechanical technology, computational fluid dynamics, software applications, and animal and plant genetics [1,2].

The ability of this intriguing area to describe dynamical systems with historical effects (memory) and strange interactions, which are frequent in the majority of natural and physical structures, is one of the major factors for the quick emergence and popularity of this fascinating topic. The traditional method of computing integer orders does not provide such possibilities since the integer-order parameter has only a limited number of degrees of freedom. The Riemann-Liouville fractional integral [3], which is a straightforward and fruitful application of the Cauchy model of repeated integrals in classical calculus, is the most frequently used in constructing a fractional-order integral. Various fractional-order integrals and derivatives techniques were made available in the latter half of this decade. It is believed that the non-singularity that occurred at one end of the Riemann–Liouville integration period served as a driving force behind the development of these technological developments. Singularities can be avoided by applying the unique ways offered [4].

Fractional calculus has emerged as a prominent area of research interest in recent years due to the challenges posed by the locally single kernel and the predicament posed by the non-singular kernel when combined with non-locality. In this regard, Caputo and Fabrizio (CF) [5] made the first effort to create the definition of fractional calculus by providing a non-singular integral (kernel) that is constructed on a decreasing smooth exponential function. They did not verify that the fractional derivative operator had a singular kernel based on the data obtained; rather, they asserted that the fractional derivative factor is suitable for a range of physical concerns. Atanagana-Baleanu (AB) proposed a strategy in [6,7] that would improve this method by replacing a smooth exponential function with an enhanced Mittag-Leffler function utilizing a single parameter. This was done to make the process more efficient. They asserted that their fractional derivative had a fractional integral since it was the anti-derivative of their operators. The Tangana–Baleanu fractional-order derivative kernel is not local nor singular. Atangana and Koca [8] demonstrate the uniqueness and existence of the fractional-order system solution by applying the concept of the AB fractional derivative to a straightforward nonlinear system. This allows them to show that the solution is one of a kind. Algahtani [9] presented the Allen-Cahn fractional theory, which included both CF and AB fractional derivatives, intending to analyze the variances in real-world problems. Studies focusing on fractional AB and CF derivatives and their science and engineering applications can be addressed in [10–17].

The propagation of mechanical vibrations and increased temperatures through solid and flexible things has been described using various mathematical models that scientists and engineers have developed. However, only some of these ideas can be considered valid because one of the criteria for a proper framework is the inclusion of the speed of advancement of thermal and mechanical waves at finite values as empirical data. The mathematical frameworks of mechanical heat conduction through elastic materials take up much space and cannot be presented on a single paper. On the other hand,

new models need to be made to find results that are very similar to in vitro experiments and are usually in line with how deformable materials work.

One of the fundamental system equations for conventional thermoelasticity, which illustrates the thermal field, is the traditional Fourier law of heat transfer rate. It might become hyperbolic-parabolic when controlled by the equations describing the displacement temperature distribution. Because of this, it follows that the response of a normal thermally elastic body to mechanical convection diffuses at an unlimited pace, which directly opposes the way physical phenomena work [18]. Since 1967, numerous models have been created, and the term "generalized thermoelastic ideas" has been given to refer to these models collectively. Compared to the field equations found in the traditional thermoelastic concept, the standard Fourier law of heat transport is substituted in Lord and Shulman's theory (LS) [19] by the Maxwell-Cattaneo equation to incorporate one relaxation time. In contrast to the conventional heat and mass transfer equations system, Green and Lindsay's framework (GL) [20] expands the dissipation inequalities and the constitutive equations, incorporating two relaxation phases. This expansion occurs in the constitutive relations.

Differential equations in which the derivative of a function is a fraction have many alternative solutions. Certain suggested analytical approaches have been made for fractional differential equations. Due to the intractable nature of most fractional problems, a growing body of research is devoted to finding numerical solutions to these difficulties. Numerous numerical solutions have been developed for fractional equations [21], including the finite difference method (FDM) [21]. Even for researchers with no background in mathematics, FDM is straightforward to master. That's why we're giving you a rundown on fractional dynamic programming (FDM) for fractional equations. Additionally, numerical solutions can be achieved by techniques such as the random walk [22], the matrix approach [23], the Adomian decomposition technique and the variational iteration methodology [24], the homotopy approximation method (HAM) [25], the homotopy perturbation strategy (HPM) [26], and so on. Several methods for approximating solutions of classical differential equations have recently been extended to solve fractional-order differential equations [27–30].

In the thermomechanical model without energy dissipation provided by Green and Naghdi [31,32], also known as the second type of GN theory, the standard Fourier law has been replaced by the thermal gradient junction of the rate of heat transfer. Temperature rate is not included in the heat transport equation, allowing undisturbed thermoelastic waves in thermoplastic material. Likewise, heat transmission is governed by the classical law and the gradient between constitutive quantities in Green and Naghdi's fourth extension to the thermoelasticity model [33]. An energy dissipation model known as the GN-III model is commonly used to describe this heat wave type. The thermoelasticity concept has been further developed using Tzou's [34–36] dual phase-lag model. According to traditional thermoelastic theory, an approximation turns the Fourier law into a Fourier law with two alternate time translations of heat fluxes and temperature gradients. Roychoudhuri [37] established an extended heat-elastic mathematical model of the standard thermoelastic theory with three-phase delays in the heat flow vector and temperature gradient. In this context, Abouelregal [38–42] used Green and Naghdi thermoelastic models to present generalized formulas for thermoelasticity with high-order time derivatives.

Both thermoelasticity and viscous thermoelasticity benefited from the application of fractional calculus theory, which prompted Povstenko [43] to propose a non-comparative quasi-static concept of thermoelasticity based on the fractional equation of thermal conductivity. The diffusion-wave equation with time-fractional derivatives was the subject of the first publication on fractional

thermoelasticity [43], which appeared in 2005. To examine the thermal stresses in an infinite elastic medium with a circular cylindrical aperture, Povstenko [44–46] used a model of thermal stresses based on the thermal conductivity equation with the time fractionional derivative of Caputo. In addition, Povstenko et al. [47] determined the solution to the time-fractional heat conduction equation for an unbounded solid with an axisymmetric heat transfer rate working in a circular domain and a circular external crack of interior radius. The time-fractional heat transfer equation with the Caputo fractional derivative is obtained by expressing the heat flux vector in terms of the Riemann-Liouville fractional integrals and derivatives of temperature gradient. Qiao et al. [48] took into account the dual-phase-lag (DPL) model's approximation of the heat transfer rate and the temperature gradient using fractional Taylor's series expansions of varying orders. They came up with the time-fractional DPL heat transfer model to help heat ultrathin gold films with femtosecond laser pulses.

Yu and Zhao [49] developed fractional thermoelastic models based on generalized Lord-Shulman and Green-Naghdi theories as well as traditional thermoelastic model. In order to investigate the transitory responses brought on by a relocating source of heat, Yu and Deng [50] constructed a unified fractional thermoelastic framework. Caputo-Fabrizio, Atangana-Baleanu, and Tempered-Caputo-type fractional derivatives are introduced to theorize fresh perspectives on fractional thermoelasticity. Under the influence of thermal shock, Xue et al. [51] utilized the unified fractional heat transfer model to examine the transient thermoelastic reactions surrounding a Griffith fracture in a half-space or strip. Assuming complete insulation along the fracture's faces, the crack runs parallel to the boundary of the half-space or strip. For microscale metals, Yu and Deng [52] theoretically derived gradient-type thermoelasticity via an electron-lattice coupling mechanism using extended thermodynamics and the heat-conducting electron-lattice framework. They in [53] developed an integrated fractional thermoelastic framework for piezoelectric devices, illuminating the impact of various formulations on transient behaviors. Theoretically, on the basis of the Cattaneo-type formula, a unified form of the fractional heat transfer law is put forth by utilizing the fractional derivatives of Caputo-Fabrizio, Atangana-Baleanu, and Tempered-Caputo.

Using fractional calculus, the effect of the fractional integral operators of Riemann-Liouville, Caputo-Fabrizio, and Atangana-Baleanu was studied in the framework of thermoelasticity of different types of heat and mass transfer models. So, the current study proposes to develop an entirely new thermoelasticity concept that incorporates fractional differentiation by employing a wide range of distinct fractional derivative operators. This fractional model (fractional DPL model) was developed based on thermoelasticity with two-phase delays. There are many thermoelastic difficulties that it is believed that this proposed fractal model can help to solve.

A thermoelasticity model was built to study the thermomagnetic behavior of solid material with a spherical cavity regularly subjected to thermal shock and immersed in a continuous axial magnetic field inside the hole. A solution has been found in the suggested Laplace transform and inversion algorithm to approximate inverse Laplace calculus. The calculated values of the temperature, tension, displacement, magnetic, and induced electric fields were depicted in a graphical view. Without the fractional derivative, several fields' response was measured and analyzed.

Using the fractional derivation of the elastic heat transfer model, three types of fractional integrals will be considered and presented in Section 2. The unique cases of the model will be discussed in the third section and its subsections. Section 4 shows how thermoplastics respond to thermal shock applied to the surface of a material containing an infinite spherical hole as an

application of the model derived in this work. In the fifth and sixth sections, the Laplace transform method and the numerical Laplace inverse are introduced to solve the ruling system of linear equations. The data was presented and analyzed in the seven sections and subsections, highlighting the most important findings. In Section VIII's last part of the study, the observations and conclusions are discussed.

2. The fractional thermoelastic model with phase lags

The governing system equations for a homogeneous material will be presented in this section. The following system of equations governs the generalized thermoelastic theory:

$$S_{ij} = 2\mu e_{ij} + [\lambda e_{kk} - \gamma\theta]\delta_{ij}, \tag{1}$$

$$2e_{ij} = U_{i,j} + U_{j,i}, \tag{2}$$

$$S_{ij,j} + R_i = \rho \frac{\partial^2 U_i}{\partial t^2}, \tag{3}$$

$$\rho C_s \frac{\partial \theta}{\partial t} + T_0 \gamma \frac{\partial e_{kk}}{\partial t} = -\nabla \cdot \vec{q} + Q, \tag{4}$$

where S_{ij} denotes the stress tensor, e_{ij} represents the strain tensor, $\gamma = (3\lambda + 2\mu)\alpha_t$ characterizes the coupling factor, α_t symbolizes the thermal expansion, λ, μ signifies the Lamé's constants, δ_{ij} indicates Kronecker's delta, e_{kk} is the cubical dilatation, $\theta = T - T_0$ is the temperature change, T denotes the absolute temperature, T_0 means the environmental temperature, U_i are the components of the displacement vector, R_i are the body force components, ρ is the density of the material, C_s signifies the specific heat, Q indicates the heat supply, $\vec{q}$ denotes the vector of the heat flux.

If Eqs (1) and (3) are combined, we get the following:

$$(\lambda + \mu)U_{j,ij} + \mu U_{i,jj} - \gamma\theta_{,i} + R_i = \rho \frac{\partial^2 U_i}{\partial t^2}. \tag{5}$$

Tzou [34–36] suggested an improved version of Fourier's law that includes a phase delay. This model, now known as the DPL model, can be summarized as follows:

$$\vec{q} + \tau_q \frac{\partial \vec{q}}{\partial t} = -K\left(1 + \tau_\theta \frac{\partial}{\partial t}\right)\nabla\theta, \tag{6}$$

where K symbolizes thermal conductivity, τ_q and τ_θ are the phase-lags.

This main part of the article will describe a new mathematical model of partial thermoelasticity. This model will include not one, not two, but three distinct types of known fractional integrals. Riemann-Liouville (RL), Caputo-Fabrizio (CF), and Atangana-Baleanu (AB) are the three different fractional operators that will be considered in this study. In previous studies and literature, fractional calculus has been used to solve various physical problems. Examples of such applications include: Many different systems can exhibit memory, date, or nonlocal effects, depending on the initial justifications given for using fractional derivative models. These models are usually difficult to explain when integer-order derivatives are used. For several decades, many scholars have developed a variety of definitions of the integral or derivative incorrect order, each using its own distinct sets of

formulas and methods. Much of the older research uses either the fractional-order Riemann–Liouville derivative or the fractional Caputo derivative.

The the Riemann-Liouville (RL) fractional derivative of order $\alpha \in \mathbb{R}^+$ can be determined as follows when applied to any real local integral function $\hbar(t)$, by [54]:

$$D_t^{(\alpha)}\hbar(t) = \frac{1}{\Gamma(1-\alpha)}\frac{d}{dt}\int_0^t \frac{\hbar(t)}{(t-\xi)^{\alpha}}\,d\xi. \tag{7}$$

For any arbitrary numbers $\alpha_1, \alpha_2 > 0$, this implies that $D_t^{(\alpha_1)}\hbar(t) \cdot D_t^{(\alpha_2)}\hbar(t) = D_t^{(\alpha_1+\alpha_2)}\hbar(t)$. For incorrect ordering operations, the Laplace transform of $D_t^{(\alpha)}\hbar(t)$ is given by

$$\mathcal{L}\left[D_t^{(\alpha)}\hbar(t)\right] = s^{\alpha}\mathcal{L}[\hbar(t)] - \sum_{k=0}^{\alpha-1} s^{\alpha-k-1}\,\hbar^{(k)}(0). \tag{8}$$

It was highlighted not so long ago that the definitions of these derivatives contain part of their kernel. This singularity occurs at the end of a predetermined period. As a direct outcome, different definitions related to completely new fractional derivatives have been presented to meet this challenge. The main differences between the different definitions of fractional derivatives lie in the cores that can be applied to meet the requirements of various applications. Some investigators have proposed modifications of the RL and Caputo derivatives. These modifications center on replacing the weak singular kernels of the RL and Caputo derivatives with some continuous non-singular functions during the interval $[0, \xi\,]$ where $\xi > 0$. These modifications aim to avoid difficulties caused by singularities.

The derivative of fractional order $\alpha \in (0,1)$ in the context of Caputo can be represented as [54]:

$$CD_t^{(\alpha)}\hbar(t) = \int_0^t \frac{1}{\Gamma(1-\alpha)(t-\xi)^{\alpha}}\,\dot{\hbar}(\tau)\,d\xi, \tag{9}$$

where $\Gamma(1-\alpha)$ symbolizes the Gamma function.

The last work of Caputo and Fabrizio (CF) [5] defines the fractional derivative with fractional order $\alpha \in (0,1)$ and an exponential kernel for the smooth function $\hbar(t)$ is as follows:

$$CFD_t^{(\alpha)}\hbar(t) = \frac{1}{1-\alpha}\int_0^t \dot{\hbar}(\xi)e^{\left(-\frac{\alpha}{(1-\alpha)}(t-\xi)\right)}\,d\xi. \tag{10}$$

The fractional Caputo and Fabrizio (CF) derivative given by the Laplace transform takes the following form:

$$\mathcal{L}\left[CFD_t^{(\alpha)}\hbar(t)\right] = \frac{1}{s+\alpha(1-s)}[s\mathcal{L}[\hbar(t)] - \hbar(0)]. \tag{11}$$

The previous studies experimentally found that the fractional derivative operator of CF cannot represent the non-singular kernel correctly. Several researchers have shown that this fractional CF-derived agent may solve various physical challenges [55]. Despite this, the CF fractional derivative presented significant challenges because the kernels in its integral were non-singular but still nonlocal. Furthermore, according to certain studies, the bound integral in the CF derivative is not a fractional operator. In this regard, Atangana and Baleanu [6,7] created fractional derivatives depending on Caputo and Riemann-Liouville notions and the enhanced Mittag-Leffler function to solve the problem of non-singularity as well as the problem of kernel non-localization. Changes in the fractional

operators and fractional differentiation orders greatly affect all the physical areas that have been looked into.

The formula that can be used to define the Atanagana-Baleanu fractional integral of order $\alpha \in (0,1)$ for $\hbar(t) \in H^1(0,b)$ with $b > 0$ is as follows: [6,7]

$$ABD_t^{(\alpha)}\hbar(t) = \frac{1}{1-\alpha}\int_0^t \dot{\hbar}(\xi)E_\alpha\left(-\frac{\alpha}{(1-\alpha)}(t-\xi)^\alpha\right)d\xi. \tag{12}$$

The function E_α is the Mittag-Leffler function. For $0 < \alpha \leq 1$, by applying the Laplace transform procedure to Eq (12), we have

$$\mathcal{L}\left[ABD_t^{(\alpha)}f(t)\right] = \frac{1}{1-\alpha}\frac{s^\alpha \mathcal{L}[f(t)] - s^{\alpha-1}f(0)}{s^\alpha + \frac{\alpha}{1-\alpha}}, \ \ s > 0. \tag{13}$$

This new fractional formula, very similar to the common use of the Caputo derivative, makes it quite straightforward. Note that if the function $\hbar(t)$ is constant, then $D_t^{(\alpha)}\hbar(t) = 0$ is zero. Unlike the previous definition of the fractional derivative, the present kernel does not contain a singularity when $t = \xi$, which is the basic distinction between the current and previous definitions. It is possible to check that the scalar derivative of the first degree is reached when it is equal to $\alpha = 1$. This value is

$$\lim_{\alpha\to 1}\left[D_t^{(\alpha)}\hbar(t)\right] = \dot{\hbar}(t). \tag{14}$$

To develop an advanced fractional model of generalized thermal elasticity, we will first perform the following substitution in modified Fourier's law (6): We will replace the partial derivatives $\frac{\partial}{\partial t}$ with respect to the instant time t with a fractional operator $D_t^{(\alpha)}$ which will result [56]:

$$\vec{q} + \tau_q\, D_t^{(\alpha)}\vec{q} = -K\left(\vec{\nabla}\theta + \tau_\theta\, D_t^{(\alpha)}\nabla\theta\right). \tag{15}$$

One of the three fractional operators (RL, CF, and AB) is denoted by the symbol $D_t^{(\alpha)}$. The linear version of the generalized heat transfer model with a fractional operator is constructed by combining the energy equations (4) and modifying Fourie's law (15), and it can be written as:

$$\left(1 + \tau_q\, D_t^{(\alpha)}\right)\left[\rho C_E\frac{\partial\theta}{\partial t} + T_0\gamma\frac{\partial e_{kk}}{\partial t} - Q\right] = \left(1 + \tau_\theta\, D_t^{(\alpha)}\right)\left(\nabla\cdot(K\,\nabla\theta)\right). \tag{16}$$

Classical electromagnetism, usual optics, and electrodynamics rely heavily on Lorentz's force law and Maxwell's equations as the basic theoretical frameworks in the field. Equations are used as mathematical concepts to describe electromagnetic, optical, and radio systems such as power generation, electric motors, transmission systems, eyeglasses, sensors, etc. These equations describe how the formation of electric and magnetic fields occurs within media due to differences in the fields and the charges and the flow of current that flows through them. By applying these mathematical formulas, Maxwell put forward the hypothesis that light is a clear example of the phenomenon of electromagnetism. A difficult set of four equations called Maxwell's equations is introduced to explain the electromagnetic universe. James Clerk Maxwell developed these equations. These equations explain the motion and behavior of magnetic and electric fields and how objects affect fields, and how they are affected by fields. The equations developed by Maxwell to describe the

electromagnetic control system can be written as [57–59]:

$$\nabla \times \vec{h} = \vec{J}, \quad -\mu_0 \frac{\partial}{\partial t}(\vec{h}) = \nabla \times \vec{E}, \quad \vec{E} = -\mu_0 \left(\frac{\partial \vec{U}}{\partial t} \times \vec{B}\right), \\ \vec{h} = \nabla \times \left(\vec{U} \times \vec{B}\right), \ \nabla \cdot \vec{h} = 0, \tag{17}$$

where $\vec{h}$ is the induced magnetic field, $\vec{E}$ is the electric field, $\vec{J}$ is the current density, $\vec{B}$ is the magnetic field, μ_0 denotes the magnetic permeability.

Maxwell stress, denoted by M_{ij} as a complement to the equations given earlier can also be calculated using the following relationship: [57,58]

$$M_{ij} = \mu_0 \left[B_i h_j + B_j h_i - B_k h_k \delta_{ij}\right]. \tag{18}$$

The Lorentz force, denoted by $\vec{L}$, can also be determined by

$$\vec{L} = \mu_0 \left(\vec{J} \times \vec{B}\right). \tag{19}$$

3. Special cases

In this section, a set of different distinct theories of thermal elasticity will be presented that can be derived as specific cases of the heat transfer rate equation with different fractal derivative operators:

3.1. Thermoelastic models

Many of the types of thermoelastic models mentioned above can be produced by ignoring the fractional differentiation ($\alpha = 1$) in the fundamental equations and based on the parameters τ_θ and τ_q.

- Coupled thermoelastic model, abbreviated as CTE, can be attained if $\tau_\theta = \tau_q = 0$.
- A model of thermoelasticity with one a single-phase lag (LS) can be obtained if $\tau_\theta = 0$, $\tau_q > 0$.
- The dual-phase-lag (DPL) thermoelasticity model can be attained if $\tau_q, \tau_\theta > 0$.

3.2. Fractional models of thermoelasticity

Using the fractional differential operators $D_t^{(\alpha)}, 0 < \alpha \leq 1$, one can derive the two fractional thermoelasticity models listed below:

- Model of fractional thermoelasticity with single-phase lag (FLS): $\tau_\theta = 0, \ \tau_q > 0$.
- The dual-phase-lag fractional thermoelasticity model (FDPL): $\tau_q, \tau_\theta > 0$.

4. Applicable problem formulation

At T_0, an infinitely homogeneous, isotropic, conductive thermoelastic material occupying the region $a \leq r \leq \infty$ and containing a spherical cavity of radius a was considered. This problem is

graphically described in Figure 1. In the absence of an external electric field, a homogeneous axial magnetic field $\vec{B} = (0,0,H_0)$ was assumed, which would have a constant value. The medium is assumed to be initially inert, while the cavity surface $r = a$ will be bound and subject to several different heat fluxes. Due to the nature of the proposed problem, consideration will be given to the spherical polar coordinate system (r, Θ, ϕ) with the origin of the coordinates determined at the center of the bore. It will be assumed that thermoelastic responses are the same around the axes. Because of this symmetry, the in-center state functions will depend only on the distance r and instant time t. Also, for condition regularity, it must be considered that all the studied field variables are restricted when $r \to \infty$.

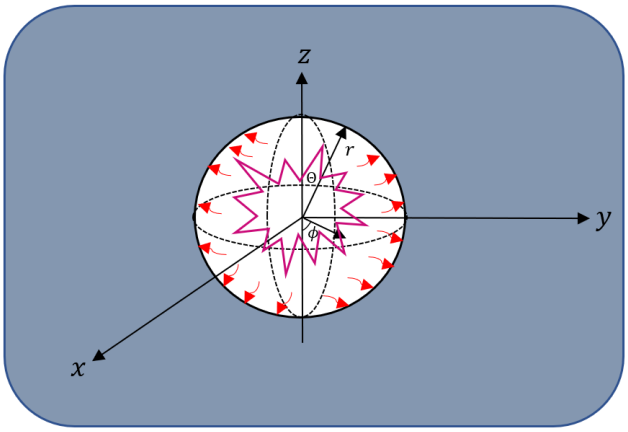

Figure 1. The configurations of a thermoelastic medium having a spherical hole.

As a result, the governing equations for the one-dimensional problem of thermoelasticity can be expressed as:

$$U_r = U(r,t),\ U_\xi(r,t) = U_z(r,t) = 0, \tag{20}$$

$$e_{rr} = \frac{\partial U}{\partial r},\ e_{\Theta\Theta} = e_{\phi\phi} = \frac{U}{r}, \tag{21}$$

$$e = \nabla \cdot U = \frac{\partial U}{\partial r} + \frac{2U}{r} = \frac{1}{r^2}\frac{\partial (r^2 U)}{\partial r}, \tag{22}$$

$$S_{rr} = 2\mu \frac{\partial U}{\partial r} + \lambda e - \gamma\theta, \tag{23}$$

$$S_{\Theta\Theta} = 2\mu \frac{U}{r} + \lambda e - \gamma\theta, \tag{24}$$

$$\frac{\partial S_{rr}}{\partial r} + \frac{2}{r}(S_{rr} - S_{\Theta\Theta}) + L_r = \rho \frac{\partial^2 U}{\partial t^2}. \tag{25}$$

Application of a fixed magnetic field vector $\vec{B} = (0,0,H_0)$ generates an induced magnetic field $\vec{h}$ in the ϕ-axis direction, as well as an induced electric field $\vec{E}$ and an electric current density $\vec{J}$ in the ξ-axis direction.

$$\vec{h} = -H_0\left(0,0,\frac{1}{r^2}\frac{\partial(r^2U)}{\partial r}\right),\ \vec{J} = -H_0\left(0,\frac{\partial e}{\partial r},0\right),\quad \vec{E} = \mu_0 H_0^2\left(0,\frac{\partial U}{\partial t},0\right). \tag{26}$$

When replacing Eq (26) with Eq (19), the radial Lorentz force L_r and the Maxwell stress components M_{rr} will be represented by the formulas

$$L_r = \mu_0\left(\vec{J}\times\vec{B}\right)_r = \mu_0 H_0^2\frac{\partial e}{\partial r},\quad M_{rr} = \mu_0 H_0^2 e. \tag{27}$$

When dealing with thermoelastic materials, the improved steady-state heat equation can be found as:

$$\nabla^2\theta + \tau_\theta D_t^{(\alpha)}(\nabla^2\theta) = \frac{1}{k}\left(1+\tau_q D_t^{(\alpha)}\right)\frac{\partial\theta}{\partial t} + \frac{\gamma T_0}{K}\left(1+\tau_q D_t^{(\alpha)}\right)\frac{\partial e}{\partial t}, \tag{28}$$

where $\frac{K}{\rho C_e} = k$.

After utilizing Eqs (23) and (24), the motion Eq (25) can be expressed as

$$\left(\frac{\lambda+2\mu}{\rho}+\frac{\mu_0 H_0^2}{\rho}\right)\frac{\partial e}{\partial r} = \frac{\gamma}{\rho}\frac{\partial\theta}{\partial r} + \frac{\partial^2 U}{\partial t^2}. \tag{29}$$

When one applies the differential operator $\frac{\partial}{\partial r}+\frac{2}{r}$ to both sides of the Eq (29), one arrives at the following result:

$$\rho(c_0^2 + a_0^2)\nabla^2 e = \gamma\nabla^2\theta + \rho\frac{\partial^2 e}{\partial t^2}. \tag{30}$$

where $\nabla^2 = \frac{1}{r^2}\frac{\partial}{\partial r}\left(r^2\frac{\partial}{\partial r}\right)$, $c_0^2 = \frac{\lambda+2\mu}{\rho}$ and $a_0^2 = \frac{\mu_0 H_0^2}{\rho}$.

To facilitate the governing equations into non-dimensional forms, we will now use the field quantities as follows:

$$\begin{gathered}\{r', U'\} = \frac{c_0}{k}\{r, U\},\ \left\{t', \tau_\theta', \tau_q'\right\} = \frac{c_0^2}{k}\left\{t, \tau_\theta, \tau_q\right\},\ \theta' = \frac{\gamma}{\rho c_0^2}\theta,\\ \left\{S_{ij}', M_{ij}'\right\} = \frac{1}{\rho c_0^2}\left\{S_{ij,} M_{rr}\right\}.\end{gathered} \tag{31}$$

When the primes are omitted from the basic equations, the non-dimensional equations have the following formulas:

$$\left(1+\tau_1 D_t^{(\alpha)}\right)\nabla^2\theta = \left(1+\tau_2 D_t^{(\alpha)}\right)\left(\frac{\partial\theta}{\partial t}+\varepsilon\frac{\partial e}{\partial t}\right), \tag{32}$$

$$\nabla^2 e = a_1\nabla^2\theta + a_2\frac{\partial^2 e}{\partial t^2}. \tag{33}$$

$$S_{rr} = 4\beta^2\frac{U}{r} + e - \theta, \tag{34}$$

$$S_{\Theta\Theta} = -2\beta^2\frac{U}{r} + (1-2\beta^2)e - \theta, \tag{35}$$

where

$$\beta^2 = \frac{\mu}{\lambda+2\mu},\ \varepsilon = \frac{T_0\gamma^2}{\rho^2 c_0^2 C_e}, a_1 = \frac{g}{c_0^2+a_0^2}, a_2 = \frac{\rho c_0^2}{c_0^2+a_0^2},$$
$$g = \frac{\gamma T_0}{\rho}, \tau_1 = \tau_\theta \left(\frac{k}{c_0^2}\right)^{\alpha-1}, \tau_1 = \tau_q \left(\frac{k}{c_0^2}\right)^{\alpha-1}. \tag{36}$$

When time t equals zero, the following are the initial conditions for the problem:

$$U(r,0) = 0 = \frac{\partial U(r,0)}{\partial r}, \theta(r,0) = 0 = \frac{\partial \theta(r,0)}{\partial r}. \tag{37}$$

In this scenario, we will suppose that the surrounding plane of the cavity, denoted by the symbol $r = a$, is subject to a moving heat flux q. The following will be a consideration of the modified Fourier law (15) with fractional order:

$$K\left(1 + \tau_\theta D_t^{(\alpha)}\right)\frac{\partial \theta}{\partial r} = -\left(1 + \tau_q D_t^{(\alpha)}\right)q \quad \text{at} \quad r = a,\ t > 0. \tag{38}$$

It will be taken into account that the heat flow q moves in the direction of the cavity axis at a constant velocity ϑ and decreases exponentially with the instant time t as shown in the following relationship [60]:

$$q = Q_0\ e^{-\omega t}\ \delta(r - vt), \qquad \omega, v > 0. \tag{39}$$

Here, we will suppose that ω and Q_0 are constants, and that $\delta(.)$ represents the Dirac delta. If we take the dimensionless quantities (31) and substitute them into Eq (38), then we obtain

$$\left(1 + \tau_1 D_t^{(\alpha)}\right)\frac{\partial \theta(\mathrm{r},t)}{\partial r} = -q_1\left(1 + \tau_2 D_t^{(\alpha)}\right)e^{-\omega t}\ \delta(r - \vartheta t),\ q_1 = \frac{q_0 \rho k c_0}{\gamma}. \tag{40}$$

It will be taken into account that mechanical constraints ensure that surface displacement is restricted. This assumption can be quantified using the following equation:

$$U(r,t) = 0 \ \text{ at } r = a. \tag{41}$$

5. Solution of the problem

The formula for calculating the Laplace transform of any function $g(r,t)$ is as follows:

$$\bar{g}(r,s) = \int_0^\infty g(r,t)e^{-st}dt, \quad s > 0. \tag{42}$$

To transform the basic equations under initial conditions (37), Laplace will be applied to the equations to get:

$$\nabla^2\bar{\theta} = \alpha_1\bar{\theta} + \alpha_2\nabla^2\bar{e}, \tag{43}$$

$$\nabla^2\bar{e} = a_2 s^2\bar{e} + a_1\bar{\theta}, \tag{44}$$

$$\bar{S}_{rr} = 4\beta^2\frac{\bar{U}}{r} + \bar{e} - \bar{\theta}, \tag{45}$$

$$\bar{S}_{\Theta\Theta} = -2\beta^2\frac{\bar{U}}{r} + (1 - 2\beta^2)\bar{e} - \bar{\theta}, \tag{46}$$

where

$$\alpha_0 = \begin{cases} \frac{s(1+s^{\alpha}\tau_2)}{(1+s^{\alpha}\tau_1)} & \text{for RL operator,} \\ \frac{s\left(1+\frac{s\tau_2}{s+\alpha(1-s)}\right)}{\left(1+\frac{s\tau_1}{s+\alpha(1-s)}\right)} & \text{for CF operator,} \\ \frac{s\left(1+\frac{s^{\alpha}\tau_2}{s^{\alpha}(1-\alpha)+\alpha}\right)}{\left(\frac{s^{\alpha}\tau_1}{s^{\alpha}(1-\alpha)+\alpha}\right)} & \text{for AB operator,} \end{cases} \tag{47}$$

with $\alpha_1 = \frac{\alpha_0}{1+\alpha_0 b}$ and $\alpha_2 = \frac{\alpha_0 \varepsilon}{1+\alpha_0 b}$.

By decoupling Eqs (43) and (44), we can get

$$\begin{aligned} \nabla^4 \bar{e} - \delta_1 \nabla^2 \bar{e} + \delta_2 \bar{e} = 0, \\ \nabla^4 \bar{\theta} - \delta_1 \nabla^2 \bar{\theta} + \delta_2 \bar{\theta} = 0, \end{aligned} \tag{48}$$

where

$$\delta_1 = \alpha_1 + s^2 a_2 + \alpha_2 a_1, \quad \delta_2 = \alpha_1 s^2 a_2. \tag{49}$$

By entering the parameters $\mu_i,\ i = 1,2$ in Eq (48), and therefore the following equation can be deduced:

$$\begin{aligned} (\nabla^2 - \mu_1^2)(\nabla^2 - \mu_2^2)\bar{e} = 0, \\ (\nabla^2 - \mu_1^2)(\nabla^2 - \mu_2^2)\bar{\theta} = 0. \end{aligned} \tag{50}$$

Where μ_1^2 and μ_2^2 are the root of the following equation

$$\mu^4 - \delta_1 \mu^2 + \delta_2 = 0. \tag{51}$$

By solving Eq (51), it is possible to deduce the roots of μ_i^2 as

$$\mu_1^2 = \frac{\delta_1 + \sqrt{\delta_1^2 - 4\delta_2}}{2},\ \mu_2^2 = \frac{\delta_1 - \sqrt{\delta_1^2 - 4\delta_2}}{2}. \tag{52}$$

Equation (50) will have a general solution, taking into account the regularity condition, as follows:

$$\bar{e} = \frac{\alpha_2}{\sqrt{r}}\left[A_1 \mu_1^2 K_{1/2}(\mu_1 r) + A_2 \mu_2^2 K_{1/2}(\mu_2 r)\right], \tag{53}$$

$$\bar{\theta} = \frac{1}{\sqrt{r}}\left[(\mu_1^2 - \alpha_1) A_1 K_{1/2}(\mu_1 r) + (\mu_2^2 - \alpha_1) A_2 K_{1/2}(\mu_2 r)\right]. \tag{54}$$

where the parameters denote the integrative coefficients A_i, where $i = 1,2,3$ and $K_{1/2}$ represents the second class of modified Bessel functions of the order of $1/2$.

By drawing from the relationship between $\bar{U}$ and $\bar{e}$ One can arrive at solving a dimensionless function of displacement provided that $\bar{U}$ is assumed to disappear when one reaches infinity. This solution can be written as:

$$\bar{U} = -\frac{\alpha_2}{\sqrt{r}}\left[A_1\mu_1 K_{3/2}(\mu_1 r) + A_2\mu_2 K_{3/2}(\mu_2 r)\right]. \tag{55}$$

The following formulas can be used to calculate stresses and solutions for the displacement $\bar{U}$:

$$\begin{aligned} xK'_{\mathrm{n}}(x) &= -xK_{\mathrm{n}+1}(x) + nK_{\mathrm{n}}(x), \\ xK'_{\mathrm{n}}(x) &= -xK_{\mathrm{n}-1}(x) - nK_{\mathrm{n}}(x). \end{aligned} \tag{56}$$

The thermal stresses can be determined with the help of the previous formula as follows:

$$\begin{aligned} \bar{S}_{rr} = \frac{1}{\sqrt{r}}\left[(\alpha_2\mu_1^2 - \mu_1^2 + \alpha_1)K_{1/2}(\mu_1 r) - \frac{4\beta^2\mu_1\alpha_2}{r}K_{3/2}(\mu_1 r)\right]A_1 + \\ \frac{1}{\sqrt{r}}\left[(\alpha_2\mu_2^2 - \mu_2^2 + \alpha_1)K_{1/2}(\mu_2 r) - \frac{4\beta^2\mu_2\alpha_2}{r}K_{3/2}(\mu_2 r)\right]A_2, \end{aligned} \tag{57}$$

$$\begin{aligned} \bar{S}_{\Theta\Theta} = \left[(\alpha_2\mu_1^2(1-2\beta^2) - \mu_1^2 + \alpha_1)K_{1/2}(\mu_1 r) + \frac{2\beta^2\mu_1\alpha_2}{r}K_{3/2}(\mu_1 r)\right]A_1 \\ + \left[(\alpha_2\mu_2^2(1-2\beta^2) - \mu_2^2 + \alpha_1)K_{1/2}(\mu_2 r) + \frac{2\beta^2\mu_2\alpha_2}{r}K_{3/2}(\mu_2 r)\right]A_2. \end{aligned} \tag{58}$$

Maxwell's stress $\bar{M}_{rr}$ in the field of the Laplace transform has the following solution:

$$\bar{M}_{rr} = \frac{a_0^2\alpha_2}{c_0^2\sqrt{r}}\left[A_1\mu_1^2 K_{1/2}(\mu_1 r) + A_2\mu_2^2 K_{1/2}(\mu_2 r)\right]. \tag{59}$$

In the transformed domain, conditions (40) and (41) can be expressed as:

$$\frac{\partial\bar{\theta}(r,s)}{\partial r} = -\frac{\alpha_0 Q_0}{\upsilon}e^{-\Omega r}, \quad \Omega = \frac{\omega+s}{\upsilon}, \; r = a, \tag{60}$$

$$\bar{U}(r,s) = 0, \qquad r = a. \tag{61}$$

To obtain the parameters A_i, $(i = 1,2)$, it is necessary to solve Eqs (60) and (61).

6. Laplace inversions

The previous section utilized the Laplace transform technique to derive the solutions of different physical fields. Then, the Laplace transforms of these field variables must be reversed so that the solutions can be transformed to the (r,t) time domain. In the present work, a well-established, practical, and accurate numerical approach will be utilized to get an inversion of the Laplace inversion for the different domains. This distinct method is based on an approach involving numerical inversion and is based on the Fourier series extension [61]. The numerical method described below can be utilized to transform any field $\bar{H}(r,s)$ in the Laplace space field into the space-time field [61]:

$$H(r,t) = \frac{e^{\xi t}}{\tau_1}\left(\frac{\bar{H}(\xi)}{2} + Re\sum_{k=1}^{N_0} e^{ik\pi t/\tau_1}\bar{H}(\xi + ik\pi/\tau_1)\right), \quad 0 \le t \le 2\tau_1, \tag{62}$$

The shortened limitless Fourier series has N_0 terms. The parameter N_0 is the number of statements that must be chosen in order to satisfy the previous formula:

$$e^{\xi t}Re\left(e^{iN_0\pi t/\tau_1}\bar{H}(\xi + iN_0\pi/\tau_1)\right) \leq \epsilon, \tag{63}$$

where ϵ is the desired precision level for a small perturbed positive integer. The free positive components must be equal to or greater than the real parts of any $\bar{H}(r,s)$ singularities. The parameter was set according to the specification [61,36]. The Mathematica programming language was used to build numerical code.

7. Verification

This section will validate and test the proposed method by identifying the known implications of which test transformation functions worked best. Our numerical reflection method will be compared with valid estimates to demonstrate the level of accuracy achieved.

As an illustration of the usefulness of the proposed numerical inversion method, we shall test it on two examples. The functions $\bar{M}(s) = \frac{1}{1+s+s^2}$ and $\bar{G}(s) = \frac{1}{s^{3/2}}e^{(-1/s)}$ are translated into $M(t) = \frac{2}{\sqrt{3}}e^{(-t/2)}\sin\left(\sqrt{3}t/2\right)$ and $G(t) = \frac{1}{\sqrt{\pi}}\sin\left(2\sqrt{t}\right)$. The parameters of $\xi = 0.421$, $N = 19$ and $t_1 = 7.5$ were used to invert the transform $\bar{M}(s)$ according to [62,63]. As shown in Table 1, the four methods exhibit varying degrees of deviation from the true value of $M(t)$ for times ranging from 0.0 to 10.0. When compared to the precise inverse Laplace transform, this approximation holds up rather well.

Table 1. Contrasting the accurate inverse Laplace transform with the numerical inversion.

t	$M(t)$		$G(t)$	
	Exact values	Computed values	Exact values	Computed values
1	0.5335070	0.5335090	0.513016	0.513018
2	0.4192800	0.41928100	0.173811	0.173811
3	0.1332430	0.13324300	-0.178818	-0.178819
4	-0.0495299	-0.04953000	-0.426980	-0.426981
5	-0.0879424	-0.08794260	-0.547985	-0.547986
6	-0.0508923	-0.05089240	-0.554397	-0.554398
7	-0.00764371	-0.00764373	-0.472197	-0.472199
8	0.01271510	0.01271510	-0.330715	-0.330715
9	0.01280470	0.01280470	-0.157643	-0.157644
10	0.00538548	0.00538549	0.0233339	0.0233339

With the improved method, high precision may be attained rapidly without excessive computation. Moreover, the programming effort for the method is low compared to other algorithms with similarly high accuracy [62,63]. Even more importantly, our inversion method may achieve significant gains in accuracy by increasing processing effort in a linear fashion. It is believed that our method is useful for a wider range of applications.

8. Numerical Results and discussions

This section will perform the numerical analysis using a new theoretical thermoelasticity model.

This model includes many fractional operators of fractional order. We will study what happens to an infinitely flexible thermoplastic solid with a spherical cavity when placed in a magnetic field of constant intensity. In addition to providing and calculating the numerical results, we will also consider the mechanical properties of the Cu material. Listed below are some of the physical properties of the proposed material [64]:

$$\rho = 8954\ \text{kg/m}^3\ , \{\lambda, \mu\} = \{7.76, 3.86\} \times 10^{10}\text{kg/ms}^2\ , H_0 = 10^7\text{Am}^{-1}$$
$$K = 386\ \text{W/mK}, \qquad C_E = 383.1\ \text{J kg/K}\ , \quad \alpha_t = 5 \times 10^{-7}\ 1/\text{K},$$
$$t = 0.12\text{s}, \qquad \mu_0 = 12.6 \times 10^{-7}\ \text{Hm}^{-1}, T_0 = 298\ \text{K}.$$

Numerical values of various physical domain variables will be approximated using the physical data provided earlier in this discussion. A series of numerical computations will be done as the distance r changes. Also, the values $Q_0 = 1$ and $\omega = 1$ are selected during these calculations. The optimization algorithms indicated in Eq (62) were applied. The differences in Maxwell's stress M_{rr}, radial and loop stresses S_{rr} and $S_{\Theta\Theta}$, radial deformation U, and dynamic temperature θ under the influence of several vital parameters have been studied.

8.1. Comparison of fractional derivative operators

The developed physical-mathematical model of the interaction between deformable and heat-exchange procedures allows us to determine the viscoelastic behavior of composite materials in the procedure during heat treatment, considering memory effects. This section includes comparisons of improved fractional operators (Caputo-Fabrizio (CF) and Atangana-Baleanu (AB)) that have been introduced in recent years with classical fractional operators (Riemann-Liouville (RL)) and usual derivatives (α=1). After analyzing the numerical data, we can conclude that elastic materials with a high degree of refraction heat up faster in heat treatment processes, which results in larger absolute values of stresses. This results in the buildup of residual stresses, which influences the development of stresses in a material when exposed to repeated thermal or mechanical stresses.

The objective of comparing fractional coefficients and conventional derivatives is to evaluate which fractional derivative approaches the oldest conventional derivative by clarifying which operators give a faster reduction of heat waves under the physical aspects. The mathematical findings of the various fields will be shown in tables to facilitate comparison when applying each of these operators.

To perform the numerical calculations, some values of the fractional-order parameter will be taken into consideration by examining the physical behavior of various physical fields according to the proposed model. The accompanying graphs show the difference in numerical values in the case of nonlocal fractional operators (AB and CF) and the conventional fractional model (RL) and the case in which the fractional differentiation disappears ($\alpha = 1$). For fixed values of $\upsilon = 5$, $\tau_q = 0.2$ and $\tau_\theta = 0.1$, and three separate values of $\alpha = 1$, 0.8, and 0.5; Figures 1–5 display the differences in radial displacement U, temperature θ, and stress components S_{rr} and $S_{\Theta\Theta}$ against radial coordinates r.

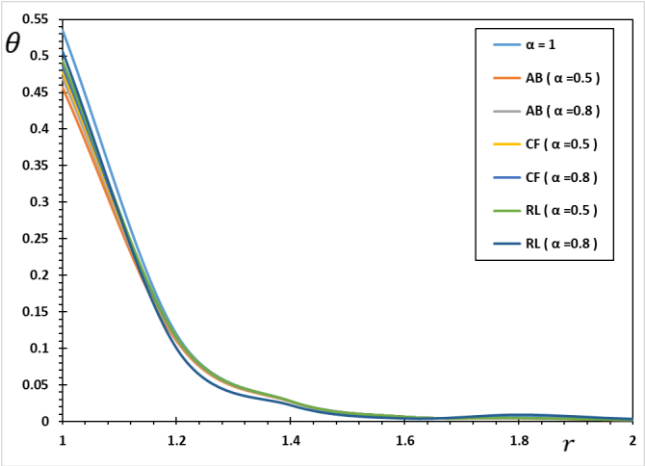

Figure 2. Variation in the temperature θ for various fractional operator.

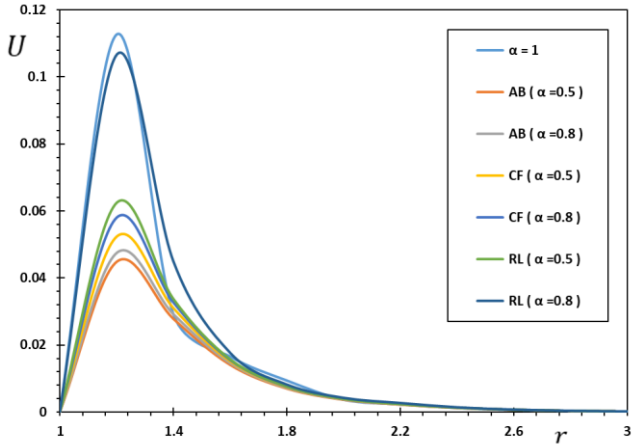

Figure 3. Variation in the displacement U for various fractional operator.

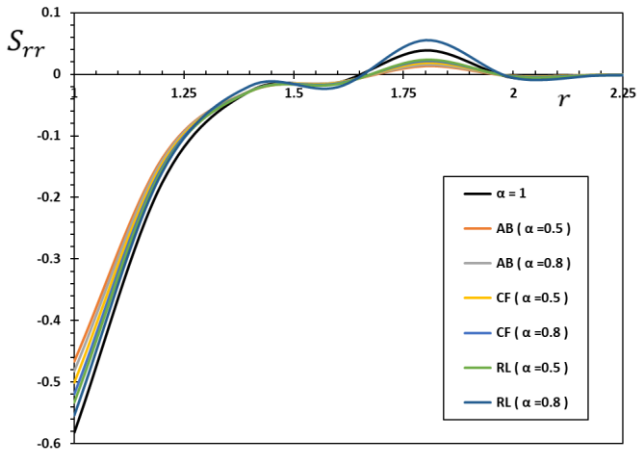

Figure 4. Variation in the radial stress S_{rr} for various fractional operator.

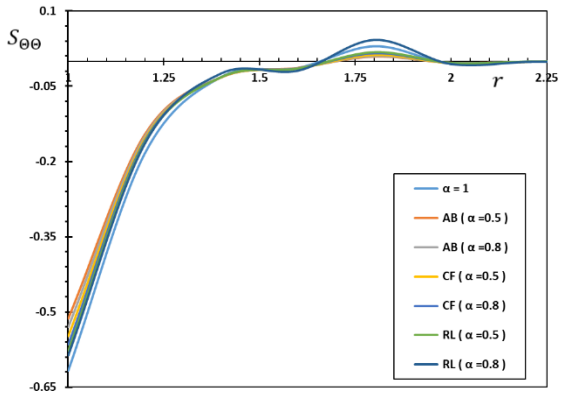

Figure 5. Variation in the hoop stress $S_{\Theta\Theta}$ for various fractional operator.

In the case of $0 < \alpha < 1$, the analysis and results of the fractional differential heat conduction model based on the fractional operator's AB, CF, and RL will be explored. From the numerical results, it is clear that the theoretical outcomes agree with the findings of the modified non-fractional thermoelastic model with the phase delay in the normal case ($\alpha = 1$) (DPL) despite the different amounts.

The computational results show that fractional differential factors significantly influence the profiles of all investigated thermophysical fields. It should also be observed that thermal and mechanical waves, both of which are stable, achieve their stable states according to the fractional order's values and the type of fractional factor. In addition, it was found that increasing the value of the fractal parameter leads to an increase in the transmission speed of the waves being investigated near the cavity surface. This is because heat flow is present at the beginning of the waves traveling through the body, but it decreases faster as the waves move deeper into the medium.

Figures 2–6 show that once the moment in time is known, the non-zero values of dynamical temperature, radial displacement, and pressure are only found within a limited area. The numerical values are all zero outside that region. This explains why the speed of heat transfer in a thermal medium is limited based on generalized models of thermoelasticity. On the other hand, conventional thermal conductivity models predict an unlimited velocity of thermal and mechanical waves. The heat-disturbed region is restricted when the time moment is given due to the finite heat diffusion velocity, leading to thermally induced displacement and stress reduction.

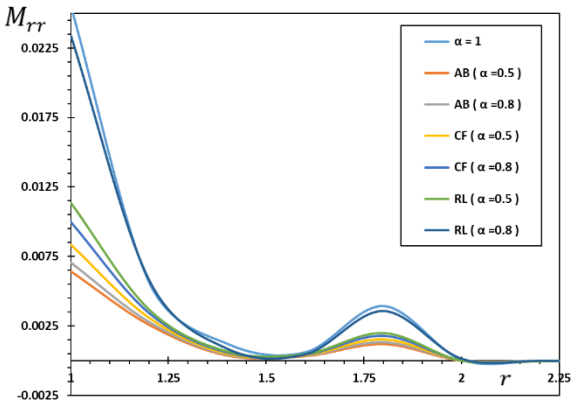

Figure 6. Variation in Maxwell's stress M_{rr} for various fractional operator.

For a set of fractional operators (AB, CF, and RL) and three values of the fractional-order parameter α, Figure 2 shows the observed changes in dynamic temperature with the position variable. It is shown in Figure 2 that the fractional order has a significant impact on the dynamics of temperature change. This can be observed by examining how the temperature θ reaches its highest value and then gradually decreases as it moves away from the cavity until it reaches zero. Thus, it can be said that the temperature distribution θ within the medium is restricted by physical processes. Other researchers study heat transfer equations without fractional differentiation, but they often forget about the problem of heat waves spreading at terminal speeds.

At $t = 0.12$, the numerical values yielded by the CF operator for the temperature distribution θ are larger than those obtained by the fractional AB operator approach. The numerical results achieved using the RL operator technique are also demonstrated to be larger than those obtained using the fractional AB, and CF approaches. Finally, a factional differential minimizes the propagation of heat waves compared to the usual situation (no fractional differentiation), as seen in Figure 2. In other words, when the fractional order falls, the thermodynamic temperature distribution decreases, and vice versa.

Figure 3 shows the change of displacement values U with space r. It can be seen from the table that the inclusion of the fractional modulus α has a significant effect on the calculated values of the displacement profile. The obtained values of the displacement distribution U decrease as the distance between any two sites within the mean grows and then decreases again until it reaches zero. In compliance with the boundary criteria, the offset variance with respect to distance always starts at zero and fades out at zero. In addition to the numerical approach, this ensures the correctness and validity of the obtained numerical results. It should also be noted that in different positions of the fractional factors (RL, CF, AB), the presence of the fractional differentiation parameter leads to a decrease in the values of the displacement U. The table also showed that a rise in the value of the fractional differentiation parameter α results in a rise in the values of the theoretical displacement. As shown in Figure 3, the partial AB model generates the smallest absolute amounts of displacement, while the standard fractional RL model gives the greatest absolute amounts of displacement.

Figures 4 and 5 illustrate the influence of the fractional differentiation factor and the various fractional operators (RL, CF, and AB) on the distributions of radial stress S_{rr} and hoop pressure $S_{\Theta\Theta}$ as the radial coordinate r varies. The tables show that the pressures start quickly with negative values, increase steadily until they reach their maximum value away from the surface of the medium gap, and decrease gradually with increasing distance until they disappear away from the turbulence region.

The computational outcomes in Figures 4 and 5 display that the amounts of thermal stresses S_{rr} and $S_{\Theta\Theta}$ are not the same when the fractional order parameters are changed. Also, depending on the type of fractional actuator used, the pressure may increase or decrease in volume. The numerical results further reveal that the stresses persist in the negative region above the cavity, and their size increases dramatically near the cavity before steadily diminishing and finally disappearing. It should also be noted that near the bore in the turbulence region, stresses usually behave in a compressive manner. It is also possible to conclude that adding a fractional differential to the thermal conductivity equation makes it difficult for mechanical waves to travel through the medium at infinite speeds, making sense based on how the problem is physically set up.

Figure 6 shows the influence of the parameter α and the fractional differentiation operators on

the Maxwell stress variance M_{rr}. The table shows that when the distance expands away from the cavity, the Maxwell stress M_{rr} dissipates rapidly, indicating that the influence of the magnetic field is instantaneous and limited. Also, as shown in the table, the fractional parameter slightly influences Maxwell stress. Moreover, the presence or absence of fractional factors has an influence, albeit insignificant, on the type and behavior as well as decreasing and increasing numerical values of Maxwell's stress M_{rr}. This is the case whether or not the fractional factors are present.

In addition, we are confident that the new fractal derivatives will play a vital role in the search for the macroscopic activity of various materials, mostly related to partial exchanges such as thermoelasticity, fluidity, and some other phenomena. When the phase delays are added to the modified heat transfer equation used to make the frame, it shows that heat waves move naturally and with a fixed size. In principle, current aerodynamic engineering issues using thermoplastic cylinders are closely related to the theory described in this work.

If everything else fails, it's possible that the fractional-order parameter could provide a new way to categorize materials in terms of their thermal conductivity. Caputo-Fabrizio integrals are linear combinations of the original function and its normal integral, and this conclusion can be drawn from their findings. When it comes to the fractional Atangan-Baleanu operator, a linear combination of the original function and Riemann-fractional Liouville's integral [4] can be used to derive it. The Atangana-Baleanu operator, which is expressed in a linear combination with the RL integrator, makes it impossible to solve many dynamical systems with just the RL integrator.

Due to the increased regularity requirements for differentiation, the CF and C operators are more suitable for use with the Caputo derivative. According to Caputo's interpretation, we first need to compute the function's derivative before we can compute the fractional derivative [13]. This is the case even if the fractional derivative is more interesting. However, in the Caputo concept, functions without first-order derivatives can have less than one fractional derivative of all orders. This contrasts with the Riemann-Liouville theorem, which states that functions without first-order derivatives cannot have fractional derivatives of any order less than one.

8.2. The influence of the speed of the heat flow

Moveable heat sources are those physical situations in which thermal excitation moves throughout the body in a more or less regular pattern concerning the heat transfer processes being studied. The problem of mobile heat sources is one of the significant studies in the process of heat conduction because of its application in various technical and other fields. Such problems can arise in various processes, including heat treatment, metal forming, casting, and smelting, as well as welding and cutting certain metals. Other applications include laser curing, metal plating, and plasma spraying.

In this subsection, the influence of the speed of a moving heat source υ on the behavior of different fields will be studied. The other physical parameters are assumed $\tau_q = 0.2$, $\tau_\theta = 0.1$, and $\alpha = 0.8$. Also, the delayed phase thermoelastic (DPL) model will be applied if only the Atangana-Baleanu (AB) fractional operator is involved in the thermal conductivity equation.

Figures 7-11 show how temperature, displacement, and thermal stresses change as a function of moving heat source velocities υ while time remains constant. We investigate three alternative heat source speeds in this scenario: $\upsilon = 3,\ 5$, and 8. The velocity of the moving heat flux is exhibited in Figures 7-11 to influence the studied field variables' fluctuations considerably.

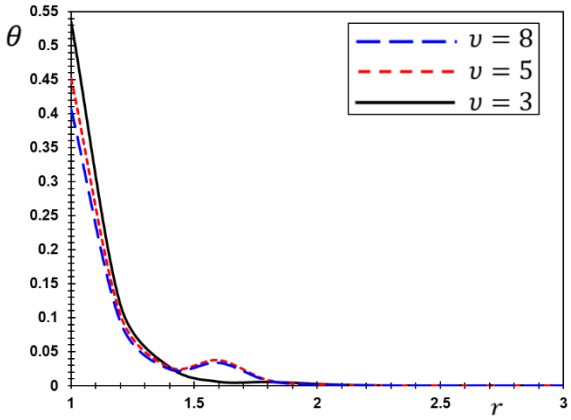

Figure 7. The temperature θ for various values of the speed υ.

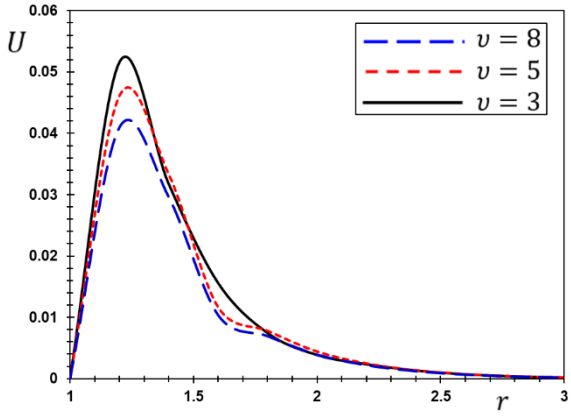

Figure 8. The displacement U for various values of the speed υ.

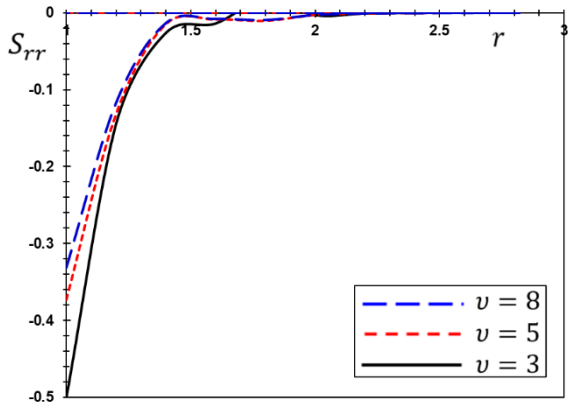

Figure 9. The stress S_{rr} for various values of the speed υ.

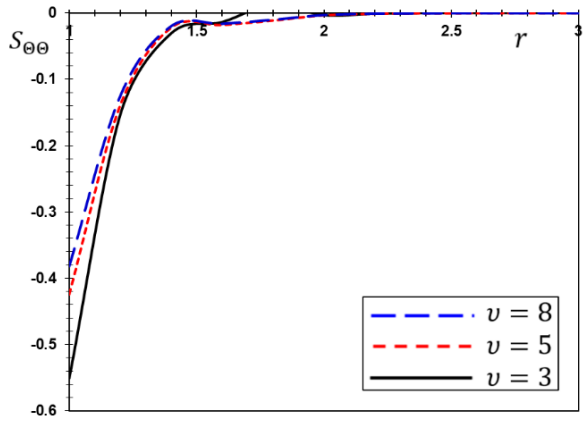

Figure 10. The stress $S_{\Theta\Theta}$ for various values of the speed υ.

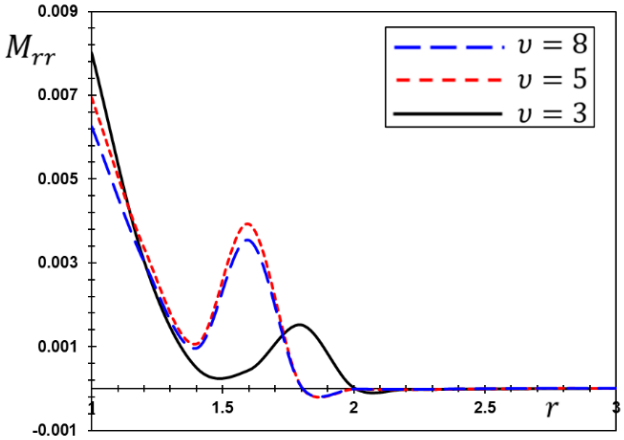

Figure 11. Maxwell's stress M_{rr} for various values of the speed υ.

Figure 7 shows the changes in thermodynamic temperature θ against radial distance r when the factor is responsible for changing the moving heat source (υ). Figure 7 shows the prominent effect of the speed of the heat flux υ on the largest temperature changes. As seen in the graph, the temperature profile surrounding the heat flux becomes time-independent sooner or later when the body is extended enough in the direction of movement. The term "quasi-steady-state condition" is used to describe this situation. As shown in the diagram, the temperature θ declines as the speed of the heat flux υ rise exponentially. This finding demonstrates that the velocities of moving heat sources are strongly correlated with temperature changes and positively affect the temperature profiles. In contrast, the wavefront effect is observed when the velocity υ of the moving heat source increases.

Equation (39) shows that the heat source simultaneously gives out the same amount of energy. But it is clear that when the velocity of the moving source rises, the amount of energy it gives out per unit length decreases. As a result, with a higher source velocity, it is found that everywhere in the thermally turbulent region receives less energy. For this reason, the local temperature distribution within the medium becomes narrower. This phenomenon has been studied in detail in [57] in line

with the results obtained.

The influence of the heat flux velocity on the displacement U variance is shown in Figure 8. As shown in the graph, parameter υ has little effect on the displacement pattern. As shown in Figure 8, the displacement U increases with time. This means the thermoelastic region develops deeper into the thermoelastic medium over time. It is also shown that thermal expansion deformation U occurs due to the applied heat source. Thermal expansion deformation U also forms over time. As a result, the rate of displacement curves rises. As the speed of the moving heat flux rises, the value of the displacement U drops, as shown in Figure 8. This occurs when the intensity of heat energy per unit length decreases at high speed. As demonstrated in Figure 8, the displacement value is maintained at zero at $r = 1$, which corresponds to the boundary conditions in that the medium is fixed in the surface cavity.

As shown in Figures 9 and 10, the radial and loop stresses change when the values of the parameter υ are increased. The presence of the parameters υ, as shown in the figures, causes the stresses to have a strong tendency to increase or decrease in amplitude. As can be seen from Figures. 9 and 10, with time, the absolute value of the tension rises. This is because the medium is bound at the surface of the gap, which prevents thermal expansion deformation along the length of the medium. Therefore, the medium is subjected to compressed thermal stresses. Absolute stresses decrease with increasing speed, as shown in Figures 9 and 10. The previous descriptions suggest a similar justification for this.

Figure 11 depicts the relationship between Maxwell stress and parameter υ. Figure 11 further shows that, as with displacement U, the factors υ have little effect on Maxwell's stress M_{rr}. This can be seen in Eq (39), which states that since the applied heat flux is moving at a constant speed υ, the distance traveled by the heat source is $r = \upsilon t$ after giving time to moment t. A rise in temperature occurs due to an increase in the amount of heat released from the source at the moment $r = \upsilon t$.

The preceding topics are limited to the most useful classical analytical solutions to trigger heat source problems that can be considered successful in practice. This means that they can be used to predict or evaluate specific findings, such as stresses produced throughout the processing of certain materials [65] and the resulting structural changes. It can also be used to investigate the evolution of a process and as a basis for reverse analysis. The most important point is that the previous results show how to conduct an analytical investigation of the problem of mobile heat sources.

The methods presented here are frequently used to solve the most difficult challenges. Some concerns regarding the non-uniform distribution pattern of a moving linear heat source [66], as well as some cases involving volumetric absorption of heat transferred by the velocity υ, as well as problems of mobile heating elements due to the finite speed of heat transfer disturbances [67–69], are not only a few of the many existing problems.

9. Conclusions

The present article studied the thermodynamic elastic responses of an infinite spheroidal medium exposed to a moving heat flux. The system of equations is formulated based on the fractional thermoelastic model with phase delay times. Also, the heat conduction equation includes multiple fractional differential operators (Riemann-Liouville, Caputo-Fabrizio, and Atangana-Baleanu), some of which are local and do not include singular kernels, and others are not. By the well-known method of Laplace transforms, differential equations are solved. Also, using an

accurate algorithm that depends on the method of approximating the Riemann sum, the approximate numerical results for temperature, displacement, and thermal stresses are obtained and displayed in tables and graphs. From the numerical results and the previous discussions, we can draw the following important conclusions:

- Computational fluid dynamics, chaos theory, epidemiology, control unit design systems, and applied physics are only a few fields in which the three fractional operators are significant.
- Changes in the fractional operators and fractional differentiation order significantly impact all physical areas investigated.
- The fractional-order parameter can be considered a new measure of the ability of elastic materials to transfer and conduct heat, similar to the thermal conductivity factor and other physical properties. Also, it is possible to study how to increase the efficiency of the thermoplastic material value by calculating the order of estimates of the fractional derivatives.
- Over time, the heat wave front moves forward at a limited pace, consistent with physical aspects. This shows that the fractional differential generalized thermal conductivity model differs significantly from the traditional Fourier law.
- According to the theoretical framework, the results of this study are closely related to the current issues of aerodynamic engineering using spherical thermoelastic domains.
- The effectiveness of the Caputo, Caputo-Fabrizio and Atangana-Baleanu operators can be demonstrated on a physical model like thermoelasticity, indicating that they can be applied to physical problems like viscoelasticity and others with confidence.
- The application of integrative-differentiation fractional-order mathematical models allows the building of new theories and models to investigate the mechanisms of stress-strain relaxation and heat transfer in fractal materials.

Researchers in mathematical insights, physics, biology, and medicine may find this study's conclusions and numerical analyses more useful when incorporating new fraction factors into their proposed models. It will be more effective when this technique is extended to other fractional factor groups (such as Atangana and Baleanu derivatives).

Acknowledgments

The authors extend their appreciation to the Deputyship for Research& Innovation, Ministry of Education, Saudi Arabia for funding this research work through the project number (QU-IF-05-03-28312). The authors also thank to Qassim University for technical support.

Conflict of interest

The authors have not disclosed any conflict of interest regarding this work's research, writing, and publication

References

1. M. Alquran, F. Yousef, F. Alquran, T. A. Sulaiman, A. Yusuf, Dual-wave solutions for the quadratic-cubic conformable-Caputo time-fractional Klein-Fock-Gordon equation, *Math. Comput. Simulat.*, **185** (2021), 62–76. https://doi.org/10.1016/j.matcom.2020.12.014

2. A. Hussanan, M. Z. Ismail, Samiulhaq, I. Khan, S. Sharidan, Radiation effect on unsteady MHD free convection flow in a porous medium with Newtonian heating, *Int. J. Appl. Math. Stat.*, **42** (2013), 474–480.
3. A. Khan, K. Ali Abro, A. Tassaddiq, I. Khan, Atangana–Baleanu and Caputo Fabrizio analysis of fractional derivatives for heat and mass transfer of second grade fluids over a vertical plate: a comparative study, *Entropy*, **19** (2017), 279. https://doi.org/10.3390/e19080279
4. A. A. Shaikh, S. Qureshi, Comparative analysis of Riemann Liouville, Caputo-Fabrizio, and Atangana-Baleanu integrals, *J. Appl. Math. Comput. Mech.*, **21** (2022), 91–101.
5. M. Caputo, M. Fabrizio, A new definition of fractional derivative without singular kernel, *Progr. Fract. Differ. Appl.*, **1** (2015), 1–13.
6. A. Atangana, D. Baleanu, New fractional derivatives with nonlocal and non-singular kernel: theory and application to heat transfer model, *Therm. Sci.*, **20** (2016), 763–769. https://doi.org/10.48550/arXiv.1602.03408
7. A. Atangana, D. Baleanu, Caputo-Fabrizio derivative applied to groundwater flow within confined aquifer, *J. Eng. Mech.*, **143** (2016), D4016005.
8. A. Atangana, I. Koca, Chaos in a simple nonlinear system with Atangana-Baleanu derivatives with fractional order, *Chaos Soliton. Fract.*, **89** (2016), 447–454. https://doi.org/10.1016/j.chaos.2016.02.012
9. O. J. J. Algahtani, Comparing the Atangana-Baleanu and Caputo-Fabrizio derivative with fractional order: Allen Cahn model, *Chaos Soliton. Fract.*, **89** (2016), 552–559. https://doi.org/10.1016/j.chaos.2016.03.026
10. H. Shatha, Atangana–Baleanu fractional framework of reproducing kernel technique in solving fractional population dynamics system, *Chaos Soliton. Fract.*, **133** (2020), 109624. https://doi.org/10.1016/j.chaos.2020.109624
11. A. Atangana, J. F. Gómez-Aguilar, Numerical approximation of Riemann–Liouville definition of fractional derivative: from Riemann–Liouville to Atangana–Baleanu, *Numer. Meth. Part. Differ. Equ.*, **34** (2018), 1502–1523. https://doi.org/10.1002/num.22195
12. T. Abdeljawad, M. A. Hajji, Q. M. Al-Mdallal, F. Jarad, Analysis of some generalized ABC-fractional logistic models, *Alex. Eng. J.*, **59** (2020), 2141–2148. https://doi.org/10.1016/j.aej.2020.01.030
13. H. Abboubakar, P. Kumar, N. A. Rangaig, S. Kumar, A malaria model with Caputo–Fabrizio and Atangana–Baleanu derivatives, *Int. J. Model. Simul. Sci.*, **12** (2021), 2150013. https://doi.org/10.1142/S1793962321500136
14. T. Sitthiwirattham, R. Gul, K. Shah, I. Mahariq, J. Soontharanon, K. J. Ansari, Study of implicit-impulsive differential equations involving Caputo-Fabrizio fractional derivative, *AIMS Math.*, **7** (2022), 4017–4037. https://doi.org/10.3934/math.2022222
15. D. Baleanu, S. S. Sajjadi, A. Jajarmi, Z. Defterli, On a nonlinear dynomical system with both chaotic and nonchaotic behaviors: a new fractional analysis and control, *Adv. Differ. Equ.*, **2021** (2021), 234. https://doi.org/10.1186/s13662-021-03393-x
16. D. Baleanu, S. S. Sajjadi, J. H. Asad, A. Jajarmi, E. Estiri, Hyperchaotic behaviors, optimal control and synchronization of a nonautonomous cardiac conduction system, *Adv. Differ. Equ.*, **2021** (2021), 175. https://doi.org/10.1186/s13662-021-03320-0

17. D. Baleanu, S. Zibaei, M. Namjoo, A. Jajarmi, A nonstandard finite difference scheme for the modeling and nonidentical synchronization of a noval fractional chaotic system, *Adv. Differ. Equ.*, **2021** (2021), 308. https://doi.org/10.1186/s13662-021-03454-1
18. R. B. Hetnarski, J. Ignaczak, Generalized thermoelasticity, *J. Therm. Stress.*, **22** (1999), 451–476. https://doi.org/10.1080/014957399280832
19. H. W. Lord, Y. Shulman, A generalized dynamical theory of thermoelasticity, *J. Mech. Phys. Solids*, **15** (1967), 229–309. https://doi.org/10.1016/0022-5096(67)90024-5
20. A. E. Green, K. A. Lindsay, Thermoelasticity, *J. Elasticity*, **2** (1972), 1–7. https://doi.org/10.1007/BF00045689
21. S. Chen, F. Liu, V. Anh, A novel implicit finite difference method for the one-dimensional fractional percolation equation, *Numer. Algor.*, **56** (2011), 517–535. https://doi.org/10.1007/s11075-010-9402-0
22. R. Metzler, J. Klafter, The random walk's guide to anomalous diffusion: a fractional dynamics approach, *Phys. Rep.*, **339** (2000), 1–77, 2000. https://doi.org/10.1016/S0370-1573(00)00070-3
23. I. Podlubny, A. Chechkin, T. Skovranek, Y. Chen, B. M. Vinagre Jara, Matrix approach to discrete fractional calculus. II. partial fractional differential equations, *J. Comput. Phys.*, **228** (2009), 3137–3153. https://doi.org/10.1016/j.jcp.2009.01.014
24. H. Jafari, A. Golbabai, S. Seifi, K. Sayevand, Homotopy analysis method for solving multi-term linear and nonlinear diffusion-wave equations of fractional order, *Comput. Math. Appl.*, **59** (2010), 1337–1344. https://doi.org/10.1016/j.camwa.2009.06.020
25. S Momani, Z. Odibat, Homotopy perturbation method for nonlinear partial differential equations of fractional order, *Phys. Lett. A*, **365** (2007), 345–350. https://doi.org/10.1016/j.physleta.2007.01.046
26. J. S. Duan, M. Li, Y. Wang, Y. L. An, Approximate solution of fractional differential equation by quadratic splines, *Fractal Fract.*, **6** (2022), 369. https://doi.org/10.3390/fractalfract6070369
27. S. K. Lydia, M. M. Jancirani, A. A. Anitha, Numerical solution of nonlinear fractional differential equations using kharrat-toma iterative method, *Nat. Volatiles Essent. Oils*, **8** (2021), 9878–9890.
28. N. A. Zabidi, Z. A. Majid, A. Kilicman, Z. B. Ibrahim, Numerical solution of fractional differential equations with Caputo derivative by using numerical fractional predict–correct technique, *Adv. Cont. Discr. Mod.*, **2022** (2022), 26. https://doi.org/10.1186/s13662-022-03697-6
29. H. Wang, F. Wu, D. Lei. A novel numerical approach for solving fractional order differential equations using hybrid functions, *AIMS Math.*, **6** (2021), 5596–5611. https://doi.org/10.3934/math.2021331
30. Z. F. Bonab, M. Javidi, Higher order methods for fractional differential equation based on fractional backward differentiation formula of order three, *Math. Comput. Simul.*, **172** (2020), 71–89. https://doi.org/10.1016/j.matcom.2019.12.019
31. A. E. Green, P. M. Naghdi, A Re-examination of the basic postulates of thermomechanics, *P. Roy. Soc. A Math. Phy.*, **432** (1991), 171–194. https://doi.org/10.1098/rspa.1991.0012
32. A. E. Green, P. M. Naghdi, Thermoelasticity without energy dissipation, *J. Elasticity*, **31** (1993), 189–208. https://doi.org/10.1007/BF00044969
33. . E. Green, P. M. Naghdi, On undamped heat waves in an elastic solid, *J. Therm. Stresses*, **15** (1992), 253–264. https://doi.org/10.1080/01495739208946136

34. D. Y. Tzou, A unified approach for heat conduction from macro- to micro-scales, *J. Heat Transfer.*, **117** (1995), 8–16. https://doi.org/10.1115/1.2822329
35. D. Y. Tzou, The generalized lagging response in small-scale and high-rate heating, *Int. J. Heat Mass Transf.*, **38** (1995), 3231–3240. https://doi.org/10.1016/0017-9310(95)00052-B
36. D. Y. Tzou, *Macro-to microscale heat transfer: the lagging behavior*, New York: Taylor & Francis, 1997.
37. S. K. Roychoudhuri, On a thermoelastic three-phase-lag model, *J. Therm. Stresses*, **30** (2007), 231–238. https://doi.org/10.1080/01495730601130919
38. A. E. Abouelregal, On Green and Naghdi thermoelasticity model without energy dissipation with higher order time differential and phase-lags, *J. Appl. Comput. Mech.*, **6** (2020), 445–456.
39. A. E. Abouelregal, Two-temperature thermoelastic model without energy dissipation including higher order time-derivatives and two phase-lags, *Mater. Res. Express*, **6** (2019), 116535. https://doi.org/10.1088/2053-1591/ab447f
40. A. E. Abouelregal, Generalized mathematical novel model of thermoelastic diffusion with four phase lags and higher-order time derivative, *Eur. Phys. J. Plus*, **135** (2020), 263.
41. A. E. Abouelregal, A novel generalized thermoelasticity with higher-order time-derivatives and three-phase lags, *Multidiscip. Model. Ma.*, **16** (2019), 689–711. https://doi.org/10.1108/MMMS-07-2019-0138
42. A. E. Abouelregal, Ö. Civalek, H. F. Oztop, Higher-order time-differential heat transfer model with three-phase lag including memory-dependent derivatives, *Int. Commun. Heat Mass*, **128** (2021), 105649. https://doi.org/10.1016/j.icheatmasstransfer.2021.105649
43. Y. Z. Povstenko, Fractional heat conduction equation and associated thermal stress, *J. Therm. Stresses*, **28** (2004), 83–102. https://doi.org/10.1080/014957390523741
44. Y. Z. Povstenko, Fractional radial heat conduction in an infinite medium with a cylindrical cavity and associated thermal stresses, *Mech. Res. Commun.*, **37** (2010), 436–440. https://doi.org/10.1016/j.mechrescom.2010.04.006
45. Y. Povstenko, Non-axisymmetric solutions to time-fractional diffusion-wave equation in an infinite cylinder, *Fract. Calc. Appl. Anal.*, **14** (2011), 418–435. https://doi.org/10.2478/s13540-011-0026-4
46. Y. Povstenko, T. Kyrylych, Fractional thermoelasticity problem for an infinite solid with a penny-shaped crack under prescribed heat flux across its surfaces, *Phil. Trans. R. Soc. A*, **378** (2020), 20190289. https://doi.org/10.1098/rsta.2019.0289
47. Y. Povstenko, T. Kyrylych, B. Woźna-Szcześniak, R. Kawa, A. Yatsko, An external circular crack in an infinite solid under axisymmetric heat flux loading in the framework of fractional thermoelasticity, *Entropy*, **24** (2022), 70. https://doi.org/10.3390/e24010070
48. Y. Qiao, X. Wang, H. Qi, H. Xu, Numerical simulation and parameters estimation of the time fractional dual-phase-lag heat conduction in femtosecond laser heating, *Int. Commun. Heat Mass*, **125** (2021), 105355. https://doi.org/10.1016/j.icheatmasstransfer.2021.105355
49. Y. J. Yu, L. J. Zhao, Fractional thermoelasticity revisited with new definitions of fractional derivative, *Eur. J. Mech. A Solid.*, **84** (2020), 104043. https://doi.org/10.1016/j.euromechsol.2020.104043
50. Y. J. Yu, Z. C. Deng, Fractional order theory of Cattaneo-type thermoelasticity using new fractional derivatives, *Appl. Math. Model.*, **87** (2020), 731–751. https://doi.org/10.1016/j.apm.2020.06.023

51. Z. Xue, J. Liu, X. Tian, Y. Yu, Thermal shock fracture associated with a unified fractional heat conduction, *Eur. J. Mech. A Solids*, **85** (2021), 104129. https://doi.org/10.1016/j.euromechsol.2020.104129
52. Y. Yu, Z. C. Deng, New insights on microscale transient thermoelastic responses for metals with electron-lattice coupling mechanism, *Eur. J. Mech. A Solid.*, **80** (2020), 103887. https://doi.org/10.1016/j.euromechsol.2019.103887
53. Y. Yu, Z. C. Deng, Fractional order thermoelasticity for piezoelectric materials, *Fractals*, **29** (2021), 2150082. https://doi.org/10.1142/S0218348X21500821
54. C. Li, F. Zeng, *Numerical methods for fractional calculus*, Boca Raton: CRC Press, 2019.
55. A. Atangana, On the new fractional derivative and application to nonlinear Fisher's reaction–diffusion equation, *Appl. Math. Comput.*, **273** (2016), 948–956. https://doi.org/10.1016/j.amc.2015.10.021
56. A. E. Abouelregal, M. Alesemi, Vibrational analysis of viscous thin beams stressed by laser mechanical load using a heat transfer model with a fractional Atangana-Baleanu operator, *Case Stud. Therm. Eng.*, **34** (2022), 102028. https://doi.org/10.1016/j.csite.2022.102028
57. N. Sarkar, A. Lahiri, Eigenvalue approach to two-temperature magneto-thermoelasticity, *Vietnam J. Math. Math.*, **40** (2012), 13–30.
58. A. Sur, Nonlocal memory-dependent heat conduction in a magneto-thermoelastic problem, *Wave. Random Complex*, **32** (2020), 251–271. https://doi.org/10.1080/17455030.2020.1770369
59. A. E. Aboueregal, H. M. Sedighi, The effect of variable properties and rotation in a visco-thermoelastic orthotropic annular cylinder under the Moore–Gibson–Thompson heat conduction model, *P. I. Mech. Eng. L J. Mat.*, **235** (2021), 1004–1020. https://doi.org/10.1177/14644207209858
60. A. E. Abouelregal, R. Alanazi, H. M. Sedighid, Thermal plane waves in unbounded nonlocal medium exposed to a moving heat source with a non-singular kernel and higher order time derivatives, *Eng. Anal. Bound. Elem.*, **140** (2022), 464–475. https://doi.org/10.1016/j.enganabound.2022.04.032
61. G. Honig, U. Hirdes, A method for the numerical inversion of Laplace transform, *J. Comput. Appl. Math.*, **10** (1984), 113–132. https://doi.org/10.1016/0377-0427(84)90075-X
62. H. Dubner, J. Abate, Numerical inversion of Laplace transforms by relating them to the finite Fourier cosine transform, *J. Assoc. Comp. Mach.*, **15** (1968), 115–123. https://doi.org/10.1145/321439.321446
63. F. R. De Hoog, J. H. Knight, A. N. Stokes, An improved method for numerical inversion of Laplace transforms, *SIAM J. Sci. Statist. Comput.*, **3** (1982), 357–366. https://doi.org/10.1137/0903022
64. A. E. Abouelregal, H. M. Sedighi, Magneto-thermoelastic behaviour of a finite viscoelastic rotating rod by incorporating Eringen's theory and heat equation including Caputo–Fabrizio fractional derivative, *Eng. Comput.*, 2022. https://doi.org/10.1007/s00366-022-01645-2
65. T. He, L. Cao, S. Li, Dynamic response of a piezoelectric rod with thermal relaxation, *J. Sound Vib.*, **306** (2007), 897–907. https://doi.org/10.1016/j.jsv.2007.06.018
66. K. Cole, J. Beck, A. Haji-Sheikh, B. Litkouhi, *Heat conduction using green's functions*, 2nd, New York: Taylor & Francis, 2010.

67. Z. B. Hou, R. Komanduri, General solutions for stationary/moving plane heat source problems in manufacturing and tribology, *Int. J. Heat Mass*, **43** (2000), 1679–1698. https://doi.org/10.1016/S0017-9310(99)00271-9
68. R. Viskanta, T. L. Bergman, *Heat transfer in materials processing*, New York: McGraw-Hill, 1998.
69. G. Araya, G. Gutierrez, Analytical solution for a transient, three-dimensional temperature distribution due to a moving laser beam, *Int. J. Heat Mass*, **49** (2006), 4124–4131. https://doi.org/10.1016/j.ijheatmasstransfer.2006.03.026

AIMS Press